https://doi.org/10.15407/ufm.25.01.003

V.A. TATARENKO*, T.M. RADCHENKO, A.Yu. NAUMUK***, and B.M. MORDYUK******

G.V. Kurdyumov Institute for Metal Physics of the N.A.S. of Ukraine,
36 Academician Vernadsky Blvd.,
UA-03142 Kyiv, Ukraine

* tatar@imp.kiev.ua, ** tarad@imp.kiev.ua,
*** artem.naumuk@gmail.com, **** mordyuk@imp.kiev.ua

STATISTICAL-THERMODYNAMIC MODELS OF THE Ni–Al-BASED ORDERING PHASES ($L1_2$, $L1_0$, $B2$): ROLE OF MAGNETIC Ni-ATOMS' CONTRIBUTION

Among known aircraft metal materials, Ni–Al is identified as an ordering intermetallic alloy with several attractive properties including low density (≅6 g/cm^3), high melting point (≅1911 K), excellent oxidation resistance (up to 1573 K), and good thermal conductivity. These and other physical properties are caused by not only the chemical composition, but also the atomic distribution over the crystal-lattice sites. The interactions between atoms of different kinds lead to deviations from their random distribution and the appearance of short-range (correlation) or even long-range (as in the case of Ni–Al) orders. The possible types of ordered phases in Ni–Al alloys are analysed through the obtained expressions for the occupation probability functions of the distribution of Ni (Al) atoms over the sites of the f.c.c. and b.c.c. lattices. The obtained expressions for the configurational free energy of ordering structures of the $L1_2$, $L1_0$, and $B2$ types take into account both the interaction of substitutional atoms on all (and not only the nearest) co-ordination spheres and the magnetism of Ni atoms. As ascertained after evaluation of the Ni–Ni exchange-interaction energy parameters for the f.c.c.-Ni–Al, the ordering of the subsystem of interacting magnetic moments of Ni atoms somewhat counteracts the long-range order.

Keywords: Ni–Al, statistical thermodynamics, long-range atomic order, 'mixing' energy, exchange interaction, magnetization.

Citation: V.A. Tatarenko, T.M. Radchenko, A.Yu. Naumuk, and B.M. Mordyuk, Statistical-Thermodynamic Models of the Ni–Al-Based Ordering Phases ($L1_2$, $L1_0$, $B2$): Role of Magnetic Ni-Atoms' Contribution, *Progress in Physics of Metals*, **25**, No. 1: 3–26 (2024)

1. Concept of Atomic Order in Ni–Al Alloys

According to the experimental phase diagram of Ni–Al-system states (Fig. 1) [1], the following 'equilibrium' macroscopic phases appear: disordered $A1$(f.c.c.)-Ni(Al)-based solid solutions, ordered (intermetallic) cubic $L1_2$(f.c.c.)-Ni_3Al and $B2$(b.c.c.)-NiAl, hexagonal $D5_{19}$-Ni_2Al_3, rhombic $D0_{11}$-$NiAl_3$ structures and (super)structures of more high rank Ni_5Al_3 (of structural Pt_5Ga_3 type) and Ni_2Al (of I_2Cd type). A feature of these ordered phases is that they retain a high degree (parameter) of atomic order (often up to the melting temperature) [2–6]. It is clear that it is caused by the high (by modulus) values of 'mixing' energies, as well as, as a consequence, a special spatial distribution of atoms and their magnetic moments in alloys with the formation of the mentioned (super) structures. On the other hand, due to a significant difference in the atomic sizes of the components and, as a result, significant local fields of deformation distortions of the average f.c.c. crystal lattice, Ni–Al alloys are prone to isostructural decomposition (if Al-atoms' concentration $c_{Al} > 0.1–0.12$) [5, 6]. Therefore, an interest in evaluating the component of 'mixing' energies corresponding to the 'strain-induced' interaction of alloying atoms arises.

As follows from experimental studies, in the f.c.c.- or b.c.c.- lattice-based alloys, the ordered phases can be formed, which are stable against to formation of antiphase boundaries (domains). Particularly, it concerns the f.c.c.-lattice-based (super)structures of $L1_2$-type (with Ni_3Al or Al_3Ni stoichiometry) and $L1_0$-type (with hypothetical Ni_2Al_2 stoichiometry in the (meta)stable state) or the b.c.c.-lattice-based (super)structure of $B2$-type (with NiAl stoichiometry). Figure 2 [7, 8] schematically reproduces the unit cells of such superstructures (at the temperature $T = 0$ K).

The f.c.c. lattice of sites in the ordered $L1_2$-type-structure alloy consists of four sublattices, one of which is formed by the vertices, and the other three are the centres of adjacent faces of the cubic unit cell, which are mainly substituted by energetically non-equivalent atoms of the first and second types, respectively. The f.c.c. lattice of sites of the ordered $L1_0$-type-structure alloy consists of two sublattices, the arrangement of their sites is represented by a system of (001) planes alternating through one. The $B2$-type layered (super)structure is formed because of the arrangement of the alternation of adjacent atomic planes; it consists of two simple cubic sublattices, which mostly contain atoms of a certain type in the sites.

The formation of an ordered, *e.g.*, $L1_2$-type, phase leads to the appearance of superstructural reflections in the diffraction pattern. These reflections for the $L1_2$ phase are defined by all three non-equivalent beams $\{\mathbf{k}_{1_X} = 2\pi\mathbf{a}_x^* = (100),\ \mathbf{k}_{2_X} = 2\pi\mathbf{a}_y^* = (010),\ \mathbf{k}_{3_X} = 2\pi\mathbf{a}_z^* = (001)\}$ of the one star of the superstructural wave vector $\mathbf{k}^X = 2\pi\mathbf{a}_z^*$ (D_{4h} group). Here,

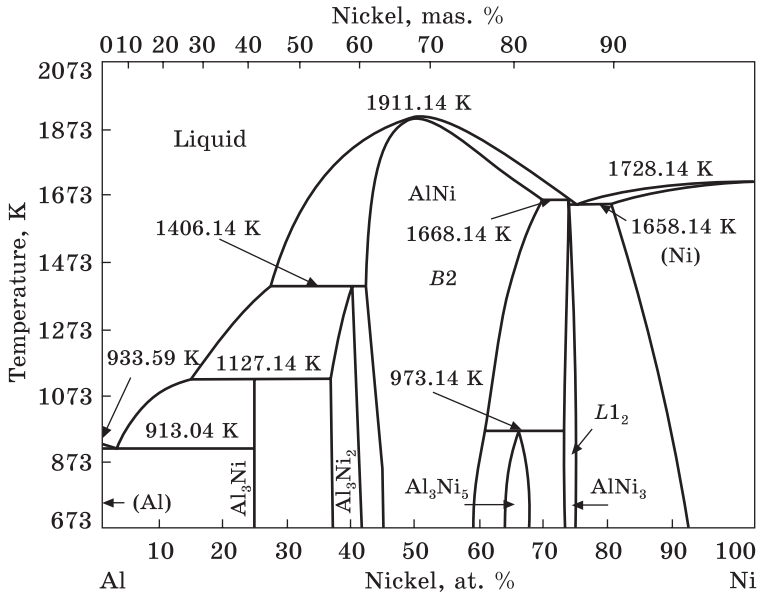

Fig. 1. Phase diagram of Ni–Al system [1]

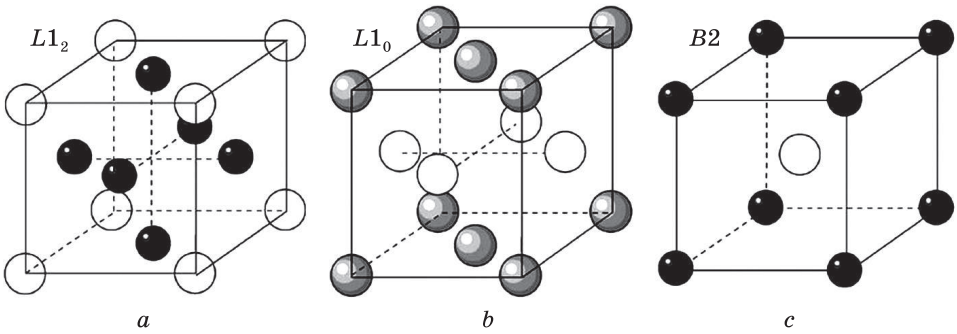

Fig. 2. Distribution of Ni and Al atoms over the sites of f.c.c. (*a*, b) and b.c.c. lattices (*c*) in the substitutional superstructures: (*a*) stoichiometric $L1_2$-type Ni_3Al or Al_3Ni, (*b*) hypothetic stoichiometric $L1_0$-type Ni_2Al_2, and (*c*) stoichiometric $B2$-type NiAl ones [7, 8]

traditionally for x-ray analysis, vectors $\mathbf{a}_x^*$, $\mathbf{a}_y^*$, $\mathbf{a}_z^*$ are the halves of main translation vectors of the reciprocal b.c.c. lattice (for the f.c.c. lattice) in the orthogonally related directions [1 0 0], [0 1 0], [0 0 1] with $|\mathbf{a}_x^*| = |\mathbf{a}_y^*| = |\mathbf{a}_z^*| = 1/a$, where a is a parameter of f.c.c. lattice of solid solution.

All other superstructure vectors in the reciprocal lattice can be obtained as a result of vector summation $(2\pi)^{-1}\mathbf{k}_{j_X}$ $(j_X = 1, 2, 3)$ with the structural vectors of the reciprocal lattice, $(2\pi)^{-1}\mathbf{B} = \sum_{n=1}^{3} h_n \mathbf{b}_n$; here,

$\{\mathbf{b}_n\}$ are three basis vectors of reciprocal lattice with integer $\{h_n\}$ numbers. Thus, indexes of all superstructural sites within the given reciprocal lattice have the form

$$\begin{aligned}
&(100) + (h_2 + h_3 - h_1; h_3 + h_1 - h_2; h_1 + h_2 - h_3) = \\
&= (h_2 + h_3 - h_1 + 1; h_3 + h_1 - h_2; h_1 + h_2 - h_3), \\
&(010) + (h_2 + h_3 - h_1; h_3 + h_1 - h_2; h_1 + h_2 - h_3) = \\
&= (h_2 + h_3 - h_1; h_3 + h_1 - h_2 + 1; h_1 + h_2 - h_3), \\
&(001) + (h_2 + h_3 - h_1; h_3 + h_1 - h_2; h_1 + h_2 - h_3) = \\
&= (h_2 + h_3 - h_1; h_3 + h_1 - h_2; h_1 + h_2 - h_3 + 1),
\end{aligned}$$

where h_1, h_2, h_3 are the indexes of structural reflections, *i.e.*, any integer numbers with $h_1 + h_2 + h_3$ being a doubled even number.

The $L1_0$-type layered superstructure can be generated by one of three non-equivalent beams $\mathbf{k}_{1X}$, $\mathbf{k}_{2X}$, or $\mathbf{k}_{3X}$ of the same star of the superstructural wave vector $\mathbf{k}^X = 2\pi\mathbf{a}_z^*$. Therefore, the $L1_0$-type ordering results in the appearance of superstructural reflections of the same type, which are determined only by, *e.g.*, $\mathbf{k}_{3X}$ vector. Other superstructural sites in such reciprocal b.c.c. lattice have indexes

$$\begin{aligned}
&(001) + (h_2 + h_3 - h_1; h_3 + h_1 - h_2; h_1 + h_2 - h_3) = \\
&= (h_2 + h_3 - h_1; h_3 + h_1 - h_2; h_1 + h_2 - h_3 + 1).
\end{aligned}$$

While the atomic long-range order (LRO) in the ordered Ni–Al alloy has been studied quite completely, the data on the short-range order (SRO) in the (dis)ordered Ni–Al alloy are practically absent. A direct method of studying the SRO is the method of diffuse scattering of x-rays. The first experimental determinations of the SRO parameters $\alpha(\mathbf{r})$ by A.A. Katsnelson with co-authors in the early 1970s showed that the Ni–Al alloy can have a SRO extending over several co-ordination shells (spheres), more than two ones, and significant contributions to the diffuse scattering of x-rays originate from various temperature- and concentration-dependent effects.

Diffuse scattering by quenched samples does not correspond to the quenching temperature, but to the state that occurs already in the quenching process. This also applies to the results of dilatometric studies and measurements of electrical resistance. Usually, such characteristics are measured for alloys, which have undergone two different heat treatments: quenching from a certain temperature followed by low-temperature annealing (heat treatment *QA*) and slow cooling (heat treatment *C*). For the *QA* heat-treated alloys, both SRO and resistivity may be greater than for the *C* heat-treated alloys. The state that occurs in hardened or cold-deformed alloys, which have undergone subsequent

low-temperature annealing, during which an increase in electrical resistance occurs, was observed by H. Thomas [9, 10] and is known to be called as the '*K*-state'. B.G. Livshits and co-authors [11, 12] put forward a hypothesis according to which the increase in electrical resistance during annealing can be explained by the formation of (nanoscale) segregations in the region of stability of a single-phase solid solution. This hypothesis was confirmed by electron-microscopy and x-ray studies [13–15] of the formation of the *K*-state in the region of stability of single-phase solid solutions for a number of nickel-based alloys. Since a greater degree of SRO can be observed in the *QA* heat treatment than in the *C* heat treatment, it is expected that the *K*-state in the alloys, in particular, may be ordered with small antiphase domains that do not coagulate in low-temperature annealing due to retardation diffusion kinetics. However, the presence of excessive vacancies, which are formed during quenching from a high temperature, still ensures a sufficiently high rate of diffusion in order to promote the formation of the *K*-state (with heat treatment *C*, there are no excessive vacancies, and, therefore, the rate of diffusion cannot ensure the formation of *K*-state). Similar consequences are expected for samples of non-equilibrium alloys, which were subjected to plastic deformation instead of hardening. In the case of heat treatment of the *QA* type, the value of the SRO parameter for the first co-ordination shell (sphere) α_I may turn out to be significantly greater than in the case of heat treatment *C*, *e.g.*, due to the fact that defects, which arise during plastic deformation, contribute to the formation of a higher degree of SRO. Additional (during heat treatment *C*) high-temperature annealing reduces the number of defects and, therefore, reduces the value of the parameter α_I, which occurs during heat treatment *QA*, but it turns out to be significantly greater than the maximum value that the composition of the alloy will allow. A.A. Katsnelson *et al.* obtained such a result for the Ni–Al alloy [16]. From this, a conclusion was made about the formation of a SRO after treatments (deformation, hardening, and irradiation) in a special way. In contrast to usual cases, the formation of SRO here is accompanied by the appearance of concentration inhomogeneities, due to which the so-called 'local' SRO is formed [17]. In the works mentioned above, despite the different terminology, the same effect of the phenomenon of structure formation is obviously meant: in some works, it is called the *K*-state; in others [17], it is called a state with 'local' SRO. This effect manifests itself in the region of a single-phase solid solution and intensifies as it approaches the solubility limit on the (quasi)equilibrium diagram.

A.G. Khachaturyan [18] proposed a physical mechanism that enables the presence of small segregations (clusters of a certain composition) corresponding to the single-phase region of the alloy equilibrium diagram. The decisive role in this mechanism is played by internal me-

chanical stresses and excessive vacancies, which arise, particularly, during hardening and plastic deformation. As shown [18], these vacancies determine not only the kinetics, but also, most importantly, the thermodynamics of the K-state. The last circumstance is the justification for the fact that the region of existence of the K-state can be plotted even on the equilibrium diagram. The idea [18] was as follows. Usually, the decomposition of a solid solution takes place due to the redistribution of atoms over the sites of a single-crystal lattice, and a mixture of two (several) phases coherently connected with each other appears [19, 20]. The coherent connection of phases with different lattice parameters leads to elastic stresses. The energy of such stresses is directly proportional to the total volume of the released phase and must be taken into account, when constructing the equilibrium diagram. Such a diagram is a diagram of metastability. Nevertheless, it is usually considered as a valid diagram of phase equilibria.

In order to predict the stability diagram [21–23], it is necessary to consider a sufficiently effective internal-stress relieving (relaxation) mechanism. Such a mechanism acts in binary alloys with an excess number of vacancies. If the inclusions of the new phase have volumes larger than the corresponding volumes of the 'holes' in the matrix, then, the diffusion of excessive vacancies to the inclusions of the new phase leads to the 'annihilation' of the excess volumes of the inclusions and, thus, to the removal internal stresses. At the same time, excessive vacancies play the role of the third component, and their number, in accordance with the usual rule of the lever, determines the total volume of inclusions of the phase that is released and is free from internal stresses. Of course, this volume is relatively small, and inclusions can be interpreted as small segregations. The region of the equilibrium diagram located between the solubility lines on the stability and metastability diagrams can be identified with the region of the presence of the K-state. In the absence of excessive vacancies (in the case of heat treatment C), the thermodynamics of the alloy is determined by the metastability diagram, and, therefore, the alloy does not undergo decomposition. In the presence of excessive vacancies (in the case of QA heat treatment), the alloy decomposes in accordance with the stability diagram. Decomposition takes place until all excessive vacancies are exhausted, allowing for the release of internal stresses. Therefore, the decomposition stops, and a heterogeneous system of segregations of a certain composition (K-state) is formed. These segregations do not grow for a long time, which is determined by the time of introduction (suction) of new vacancies from the crystal surfaces. For example, the coalescence of segregations due to the introduction of vacancies from the surfaces can occur during the experiment, *e.g.*, with an annealing time of several tens of days at temperatures even much higher than room temperature. As stated in

Ref. [18], the region of the K-state controlled by vacancies should be located on the diagram from the side of the component that has a smaller 'atomic' (ionic) radius (then, the excessive volume of the phase that is released can 'annihilate' with excessive vacancies). This conclusion should be confirmed for those systems, whose electron-microscopy studies show the presence of segregations, which do not undergo noticeable coalescence, in particular, Ni–Al [24], Ni–Mo [14, 15] and Fe–Al [13] based on nickel and iron, respectively. The fact that direct observation of stable segregations occurred precisely for these alloys (and others) only confirms these regularities. The crystal-chemical atomic radius of Fe (0.126 nm) and the metallic (crystal-chemical) radius of Ni (0.124 (0.125) nm) are significantly smaller than the metallic atomic radius of Al (0.143 nm) and the metallic (crystal-chemical) radius of Mo (0.139 (0.136) nm). The tendency, *e.g.*, of the Ni–Al alloy to generate within it a significant number of excessive 'structural' vacancies due to a significant difference in the 'atomic' radii of the components and the entropy effect is often noted by its inclusion into the class of extraction alloys. Other works also covered relevant studies; particularly, see Refs. [25–29], as well as reviews [30–32] and bibliography therein.

2. Probability Functions of Atomic Distribution and Configurational Internal Energies and Entropies of the Ordered $L1_2$-, $L1_0$-, and $B2$-Type Superstructures

Let us consider a substitutional solid solution with N_A and N_B atoms of two kinds, A (main component) and B (alloying component), respectively, which can be (re)distributed over $N = N_A + N_B$ sites of the certain rigid lattice, which is commonly known in the literature as the Ising lattice.

The configurational Hamiltonian dependent on the interatomic interactions in paramagnetic-state alloy reads as

$$\Delta H_{\text{prm}} = \frac{1}{2}\sum_{\mathbf{r},\mathbf{r}'}\Big[W^{AA}(\mathbf{r},\mathbf{r}')c_A(\mathbf{r})c_A(\mathbf{r}') + W^{BB}(\mathbf{r},\mathbf{r}')c_B(\mathbf{r})c_B(\mathbf{r}') + 2W^{AB}(\mathbf{r},\mathbf{r}')c_A(\mathbf{r})c_B(\mathbf{r}')\Big],$$

where $W^{AA}(\mathbf{r},\mathbf{r}')$, $W^{BB}(\mathbf{r},\mathbf{r}')$, $W^{AB}(\mathbf{r},\mathbf{r}'')$ are non-magnetic ('electrochemical', strain-induced [33], *etc.*) interaction energies of two atoms A, two atoms B, and two atoms A and B, respectively, located at the $\mathbf{r}$ and $\mathbf{r}'$ sites of the Ising lattice. Values $c_A(\mathbf{r})$ are random functions possessing the magnitude 1 or 0 depending on the occupation of $\mathbf{r}$ site by the A or B atom, respectively (and *vice-versa* on the analogy of $c_B(\mathbf{r})$).

Using the obvious relations $c_A(\mathbf{r}) + c_B(\mathbf{r}) \equiv 1$ and

$$\sum_{\mathbf{r}} c_B(\mathbf{r}) = N^B,$$

as well as the condition of crystallographic equivalence of all sites of the Ising lattice, we obtain the expression [34]:

$$\Delta H_{\text{prm}} = \Delta H_{0\text{prm}}^{A-B} + \frac{1}{2}\sum_{\mathbf{r},\mathbf{r}'} w_{\text{prm}}(\mathbf{r},\mathbf{r}')\, c_B(\mathbf{r})\, c_B(\mathbf{r}'),$$

where $w_{\text{prm}}(\mathbf{r},\mathbf{r}') \equiv W^{AA}(\mathbf{r},\mathbf{r}') + W^{BB}(\mathbf{r},\mathbf{r}') - 2W^{AB}(\mathbf{r},\mathbf{r}')$ are so-called 'mixing' energies $w(\mathbf{r},\mathbf{r}')$ of A and B atoms in the paramagnetic state of alloy;

$$\Delta H_{0\text{prm}}^{A-B} = \frac{1}{2}(N - 2N^B)\tilde{W}^{AA}(\mathbf{0}) + N^B\tilde{W}^{AB}(\mathbf{0}),$$

$$\tilde{W}^{AA(B)}(\mathbf{0}) = \sum_{\mathbf{r}'} W^{AA(B)}(\mathbf{r},\mathbf{r}').$$

The random value $c_B(\mathbf{r})$ characterizes the distribution of substitutional atoms over the Ising-lattice sites. The statistical-thermodynamic description within the (correlation-free) self-consistent field approximation can be carried out using the single-particle function $P(\mathbf{R}) \equiv \langle c_B(\mathbf{R})\rangle$. This function denote the probability of finding an atom of B type at the site of a primitive unit cell with the origin at the point $\mathbf{R}$ of the Ising lattice based on the Bravais lattice (the symbol $\langle ... \rangle$ denotes the averaging procedure by the canonical Gibbs ensemble) [34].

If the 'mixing' energies $w(\mathbf{r},\mathbf{r}') = w(\mathbf{R} - \mathbf{R}')$ corresponding to pairwise interatomic interactions are different from zero only for the nearest neighbours, and the sites form a simple Bravais lattice, then, this is the so-called classical Ising model for a binary alloy.

As known, within the self-consistent field approximation, the statistical thermodynamics of alloy is defined by several energy parameters of interatomic interactions [34], *viz.*, $\tilde{w}(\mathbf{0})$, $\tilde{w}(\mathbf{k}_1)$, ..., $\tilde{w}(\mathbf{k}_s)$, ..., $\tilde{w}(\mathbf{k}_{M-1})$, which are the Fourier components of 'mixing' energies,

$$\tilde{w}(\mathbf{k}) = \sum_{\mathbf{R}'} w(\mathbf{R} - \mathbf{R}')e^{-i\mathbf{k}\cdot(\mathbf{R}-\mathbf{R}')},$$

in the point $\mathbf{k}^{\Gamma} = \mathbf{0}$ (in the structural site of the reciprocal space) and in the points $\mathbf{k}_1$, $\mathbf{k}_2$, ..., $\mathbf{k}_s$, ..., $\mathbf{k}_{M-1}$ (in the superstructural sites of the reciprocal space), which belong to the first Brillouin zone (*BZ*) and the stars s of different wave vectors. The number of these parameters equals to the number of sublattices, M, on which the Ising lattice is subdivided, when the ordering occurs. For the f.c.c.-lattice-based solid solutions, such key energy parameters are $\tilde{w}(\mathbf{k}_s)$ and $\tilde{w}(\mathbf{0})$, where $\mathbf{k}_s(k_1k_2k_3)$ are $\mathbf{k}_{1_X} = 2\pi\mathbf{a}_1^*$, $\mathbf{k}_{2_X} = 2\pi\mathbf{a}_2^*$, or $\mathbf{k}_{3_X} = 2\pi\mathbf{a}_3^*$, *i.e.*, belongs to the X-star of the wave vector, which corresponds to the point (100) (either (010) or (001)) of the reciprocal space of the f.c.c. lattice and 'generates' [34] $L1_2$ or $L1_0$-type (super)structures. In case of the b.c.c.-lattice-based solid solutions stable against to fragmentation on antiphase domains, such the energy parameters are $\tilde{w}(\mathbf{k}_s)$ and $\tilde{w}(\mathbf{0})$, where the wave vector $\mathbf{k}_s(k_1k_2k_3)$

is $\mathbf{k}_{1_H} = 2\pi(\mathbf{a}_1^* + \mathbf{a}_2^* + \mathbf{a}_3^*)$ (or $\mathbf{k}_{1_P} = \pi(\mathbf{a}_1^* + \mathbf{a}_2^* + \mathbf{a}_3^*)$), *i.e.*, belongs to the stars of wave vectors $\mathbf{k}^H$ (or $\mathbf{k}^P$) corresponding to the high-symmetry point (111) (or (1/2 1/2 1/2)) of the reciprocal space of b.c.c. lattice and 'generates' [34], *e.g.*, the $B2$-type (super)structure. In these cases, $\mathbf{a}_1^*$, $\mathbf{a}_2^*$, $\mathbf{a}_3^*$ are the basis translation vectors of the reciprocal lattice along the ⟨100⟩, ⟨010⟩, and ⟨001⟩ directions, respectively.

Below, correlations in the mutual arrangement of atoms will not be taken into account. Using the static concentration waves' method [34], one can obtain the distribution of the probabilities of substitution of sites by the atoms of alloying component for the f.c.c.-lattice-based $L1_2$-type, f.c.c.-lattice-based $L1_0$-type, and b.c.c.-lattice-based $B2$-type (super) structures in Ni–Al alloys [8, 32]:

$$L1_2: \; P(\mathbf{R}) = c_B + \frac{\eta}{4}\left[\exp(i2\pi\mathbf{a}_1^* \cdot \mathbf{R}) + \exp(i2\pi\mathbf{a}_2^* \cdot \mathbf{R}) + \exp(i2\pi\mathbf{a}_3^* \cdot \mathbf{R})\right];$$

$$L1_0: \; P(\mathbf{R}) = c_B + \frac{\eta}{2}\exp(i2\pi\mathbf{a}_1^* \cdot \mathbf{R});$$

$$B2: P(\mathbf{R}) = c_B + \frac{\eta}{2}\exp\left(i2\pi(\mathbf{a}_1^* + \mathbf{a}_2^* + \mathbf{a}_3^*) \cdot \mathbf{R}\right).$$

Here, $c_B = N_B/N$ is a relative concentration of substitutional element B in the cubic crystal based on the A-component lattice; η is a LRO parameter.

If, within the self-consistent field approximation, we substitute the distribution functions $P(\mathbf{R})$ into the expression of the configurational internal energy of alloy with pair interatomic interactions [34],

$$\Delta U_{\text{conf}} = \left\langle \Delta H_{\text{prm}} \right\rangle \cong \Delta U_{0\text{conf}} + \frac{1}{2}\sum_{\mathbf{R}}\sum_{\mathbf{R}'} w(\mathbf{R} - \mathbf{R}')P(\mathbf{R})P(\mathbf{R}'),$$

where $\Delta U_{0\text{conf}} = \langle \Delta H_{0\text{prm}}^{A-B} \rangle$, and into the configurational entropy [34],

$$\Delta S_{\text{conf}} \cong -k_B \sum_{\mathbf{R}} \left[P(\mathbf{R}) \ln P(\mathbf{R}) + \left(1 - P(\mathbf{R})\right) \ln\left(1 - P(\mathbf{R})\right) \right],$$

where k_B is the Boltzmann constant, then, the expressions for configurational internal energy and entropy of $L1_2$-, $L1_0$-, and $B2$-type (super) structures in paramagnetic state are as follow, respectively:

$$\Delta U_{\text{conf}} \cong \Delta U_{0\text{conf}} + \frac{N}{2}\left[\tilde{w}(\mathbf{0})c_B^2 + \frac{3}{16}\eta^2\tilde{w}(\mathbf{k}^X)\right],$$

$$\Delta S_{\text{conf}} \cong -\frac{k_B N}{4}\left[3\left(c_B - \frac{\eta}{4}\right)\ln\left(c_B - \frac{\eta}{4}\right) + 3\left(1 - c_B + \frac{\eta}{4}\right)\ln\left(1 - c_B + \frac{\eta}{4}\right) + \right.$$

$$\left. + \left(c_B + \frac{3}{4}\eta\right)\ln\left(c_B + \frac{3}{4}\eta\right) + \left(1 - c_B - \frac{3}{4}\eta\right)\ln\left(1 - c_B - \frac{3}{4}\eta\right)\right];$$

$$\Delta U_{\text{conf}} \cong \Delta U_{0\text{conf}} + \frac{N}{2}\left[\tilde{w}(\mathbf{0})c_B^2 + \frac{1}{4}\eta^2\tilde{w}(\mathbf{k}^X)\right],$$

$$\Delta S_{\text{conf}} \cong -\frac{k_B N}{2}\left[\left(c_B - \frac{\eta}{2}\right)\ln\left(c_B - \frac{\eta}{2}\right) + \left(1 - c_B + \frac{\eta}{2}\right)\ln\left(1 - c_B + \frac{\eta}{2}\right) + \right.$$

$$\left. + \left(c_B + \frac{\eta}{2}\right)\ln\left(c_B + \frac{\eta}{2}\right) + \left(1 - c_B - \frac{\eta}{2}\right)\ln\left(1 - c_B - \frac{\eta}{2}\right)\right];$$

$$\Delta U_{\text{conf}} \cong U_{0\text{conf}} + \frac{N}{2}\left[c_B^2\tilde{w}(\mathbf{0}) + \frac{1}{4}\eta^2\tilde{w}(\mathbf{k}^H)\right],$$

$$\Delta S_{\text{conf}} \cong -\frac{k_B N}{2}\left\{\left(c_B + \frac{\eta}{2}\right)\ln\left(c_B + \frac{\eta}{2}\right) + \left(1 - c_B - \frac{\eta}{2}\right)\ln\left(1 - c_B - \frac{\eta}{2}\right) + \right.$$

$$\left. + \left(c_B - \frac{\eta}{2}\right)\ln\left(c_B - \frac{\eta}{2}\right) + \left(1 - c_B + \frac{\eta}{2}\right)\ln\left(1 - c_B + \frac{\eta}{2}\right)\right\}.$$

Energy parameters $\tilde{w}(\mathbf{0})$, $\tilde{w}(\mathbf{k}^X)$, and $\tilde{w}(\mathbf{k}^H)$ are the Fourier components of 'mixing' energies for structural $(\mathbf{k} = \mathbf{0})$ and superstructural ($\mathbf{k}^X$ and $\mathbf{k}^H$) wave vectors. It is important that these values contain 'mixing' energies $w(\mathbf{r})$ for all interatomic distances $\mathbf{r}$ in the lattice, *i.e.*, take into account interaction of all atoms in the system, but not those located within the first or several nearest co-ordination shells only.

The LRO-parameter equilibrium value, η_{eq}, for each of (super)structural type can be determined from the equality to zero of the 1st derivative of free energy: $\delta\Delta F_{\text{conf}}/\delta\eta = \delta(\Delta U_{\text{conf}} - T\Delta S_{\text{conf}})/\delta\eta = 0$. This condition results in the transcendental equations of equilibrium for $L1_2$-, $L1_0$-, and $B2$-type (super)structures, respectively:

$$\ln\left[\left(c_B - \frac{\eta_{\text{eq}}}{4}\right)\left(1 - c_B - \frac{3\eta_{\text{eq}}}{4}\right)\right] - \ln\left[\left(c_B + \frac{3\eta_{\text{eq}}}{4}\right)\left(1 - c_B + \frac{\eta_{\text{eq}}}{4}\right)\right] \cong \frac{\tilde{w}(\mathbf{k}^X)}{k_B T}\eta_{\text{eq}};$$

$$\ln\left[\left(c_B - \frac{\eta_{\text{eq}}}{2}\right)\left(1 - c_B - \frac{\eta_{\text{eq}}}{2}\right)\right] - \ln\left[\left(c_B + \frac{\eta_{\text{eq}}}{2}\right)\left(1 - c_B + \frac{\eta_{\text{eq}}}{2}\right)\right] \cong \frac{\tilde{w}(\mathbf{k}^X)}{k_B T}\eta_{\text{eq}};$$

$$\ln\left[\left(c_B - \frac{\eta_{\text{eq}}}{2}\right)\left(1 - c_B - \frac{\eta_{\text{eq}}}{2}\right)\right] - \ln\left[\left(c_B + \frac{\eta_{\text{eq}}}{2}\right)\left(1 - c_B + \frac{\eta_{\text{eq}}}{2}\right)\right] \cong \frac{\tilde{w}(\mathbf{k}^H)}{k_B T}\eta_{\text{eq}}.$$

The condition $\partial^2\Delta F_{\text{conf}}/\partial\eta^2 = 0$ yields equation for the bifurcation point:

$$T_c \approx -\frac{\tilde{w}(\mathbf{k}^{X(H)})}{k_B}c_B(1 - c_B),$$

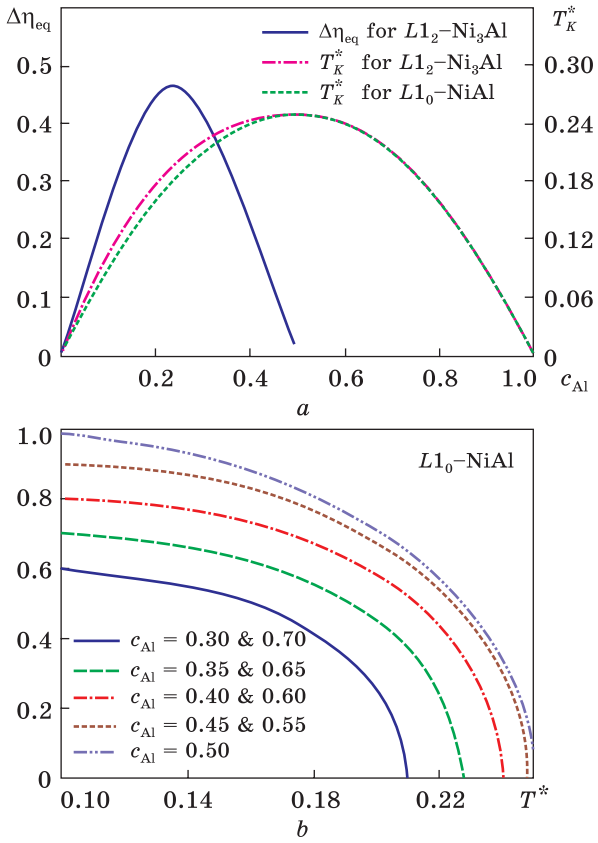

Fig. 3. Concentration dependences of the jump of the long-range atomic-order parameter at the virtual (Kurnakov's) disorder–order phase-transformation temperature T_K and the latter T^*_K (reduced T_K) for $L1_2$-Ni_3Al-type (or $L1_2$-Al_3Ni-type if c_{Ni} denotes the abscissa axis) structure and $L1_0$-NiAl-type one (*a*); equilibrium long-range atomic-order parameter *vs.* the reduced temperature at different compositions of $L1_0$-NiAl (*b*) [31]

where T_c is a temperature of 'loss of stability' of disordered solid solution with respect to the formation of certain (super)structure.

Analysis, *e.g.*, of the first equation of equilibrium, shows that the disorder–order phase transformation into $L1_2$-Ni_3Al-type (Al_3Ni-type) structure should be a 1st-order phase transition. Solving set of equations, which includes both the first equation of equilibrium and the condition of equilibrium 1st-order phase transition, $\{\Delta F(\Delta\eta, T_K) - \Delta F(0, T_K)\} = 0$, we obtain the concentration dependences of the equilibrium LRO parameter jump $\Delta\eta_{eq}$ and reduced (Kurnakov's) temperature of the order–disorder phase transformation $T_K = k_B T_K / |\tilde{w}(\mathbf{k}^X)|$ for the $L1_2$-Ni_3Al-type structure (Fig. 3, *a*) [31]. The same curves are valid as a result of the numerical solution of the set of equations for $L1_2$-Al_3Ni-type structure, if abscissa denotes relative concentration of Ni, $c_{Ni} = N_{Ni}/N$. Comparatively small LRO-parameter jump at T_K, *viz.*, $\Delta\eta_{eq}(c_{Al})|_{TK} \leq 0.467$, for $L1_2$-Ni_3Al-type (super)structure indicates that this ordered phase is stable with respect to the disordered one (*i.e.*, only with SRO). In addition, to some extent, it justifies the neglect of correlation effects in the

atomic arrangement (at least, near the order–disorder phase transformation temperature).

Analysis of the equilibrium equation and $\Delta F(\Delta\eta, T_K) = \Delta F(0, T_K)$ shows that the disorder–order phase transformation into the $L1_0$-NiAl-type structure should be a 1st-order phase transition but closer to the 2nd-order, because the LRO-parameter jump is practically unseen at the curves in Fig. 3, *b*.

3. Taking into Account of Ni-Atoms' Magnetism

The presence of the magnetic moments of Ni atoms complicates the statistical-thermodynamic analysis of the nickel alloys. In the case of the Ni–Al alloy, only Ni atoms possess the magnetism (Al is weakly paramagnetic); so, the analysis is reduced to the model of a binary alloy with one magnetic component. Reviewing the literature data on the values of magnetic moments of atoms within the Ni–Al alloys, including ordered and stoichiometric one, Ni atoms have magnetic moments of $0.604\mu_B$ or $0.616\mu_B$ according to different data (μ_B is the Bohr magneton; magnetic moments can be estimated from experiments on saturation magnetization or by the method of magnetic elastic scattering of polarized neutrons [35–38]). Thus, we expect to assume that the spin for Ni atoms $s_{\text{Ni}} = 1/2$ is more realistic as compared to $s_{\text{Ni}} = 1$.

Let us use the Heisenberg model of localized spins (neglecting the magnetism of collectivized electrons at $T > 0$ K). Then, the Hamiltonian of the spin subsystem is

$$\hat{H}_{\text{sp}} \approx \frac{1}{2}\sum_{\mathbf{R}}\sum_{\mathbf{R}'} J_{\text{NiNi}}(\mathbf{R}-\mathbf{R}')(\hat{S}_{\mathbf{R}}\cdot\hat{S}_{\mathbf{R}'})c_{\mathbf{R}}c_{\mathbf{R}'},$$

where $J_{\text{NiNi}}(\mathbf{R}-\mathbf{R}')$ is an exchange integral of two Ni ions at the sites $\mathbf{R}$ and $\mathbf{R}'$; $\hat{S}_{\mathbf{R}}$ and $\hat{S}_{\mathbf{R}'}$ denote the operators of total spin at the sites $\mathbf{R}$ and $\mathbf{R}'$, respectively; here, $c_{\mathbf{R}}$ is a random value equal to 1 or 0 depending on the atom Ni or Al occupies the site $\mathbf{R}$. The multiplier $c_{\mathbf{R}}c_{\mathbf{R}'}$ takes into account the fact that only Ni-ions' pairs contribute to the exchange energy. Averaging over all spin orientations at the sites $\{\mathbf{R}\}$ results in the model configurational Hamiltonian:

$$H_{\text{sp}} = \langle\hat{H}_{\text{sp}}\rangle_{\text{sp}} \cong \frac{1}{2}\sum_{\mathbf{R}}\sum_{\mathbf{R}'} J_{\text{NiNi}}(\mathbf{R}-\mathbf{R}')\langle(\hat{S}_{\mathbf{R}}\cdot\hat{S}_{\mathbf{R}'})\rangle_{\text{sp}}c_{\mathbf{R}}c_{\mathbf{R}'},$$

where $\langle(\ldots)\rangle_{\text{sp}} = \text{Tr}\{(\ldots)\exp[-\hat{H}_{\text{sp}}/(k_BT)]\}/\text{Tr}\exp[-\hat{H}_{\text{sp}}/(k_BT)]$ is an average over thermodynamic ensemble of interacting spins. Within the Weiss 'molecular' (*per se* mean self-consistent) field approximation,

$$\langle\hat{S}_{\mathbf{R}}\hat{S}_{\mathbf{R}'}\rangle_{\text{sp}} \cong (\langle(\hat{S}_{\mathbf{R}}\cdot\hat{S}_{\mathbf{R}'})\rangle_{\text{sp}}) \cong s_{\text{Ni}}^2\,\sigma^2(1-\delta_{\mathbf{R},\mathbf{R}'}),$$

$\langle\hat{S}_{\mathbf{R}}\rangle_{\text{sp}} \equiv s_T$ is an averaged spin moment per Ni ion with a total spin s_{Ni}, and $\sigma \equiv s_T/s_{\text{Ni}}$ is a reduced magnetization of alloy at the given composition and temperature T; $\delta_{\mathbf{R},\mathbf{R}'}$ is the Kronecker symbol.

Using two last expressions and self-consistent field approximation, the magnetic internal energy is

$$\Delta U_{\text{magn}} \cong \frac{1}{2}\sum_{\mathbf{R},\mathbf{R}'} J_{\text{NiNi}}(\mathbf{R}-\mathbf{R}')s_{\text{Ni}}^2\sigma^2\left(1-P(\mathbf{R})\right)\left(1-P(\mathbf{R}')\right),$$

where $P(\mathbf{R})$ is the above-mentioned probability functions. Then the total configurational-dependent part of the internal energy is

$$\Delta U_{\text{conf}} = \Delta H_0^{\text{Ni-Al}} + \frac{1}{2}\sum_{\mathbf{R},\mathbf{R}'} w_{\text{tot}}(\mathbf{R}-\mathbf{R}')P(\mathbf{R})P(\mathbf{R}'),$$

where

$$w_{\text{tot}}(\mathbf{R}-\mathbf{R}') = w(\mathbf{R}-\mathbf{R}') + J_{\text{NiNi}}(\mathbf{R}-\mathbf{R}')s_{\text{Ni}}^2\sigma^2$$

has a sense of the total 'mixing' energy; $w(\mathbf{R}-\mathbf{R}')$ are the mixing energies of Al and Ni atoms in a paramagnetic state. Including of the magnetism into the internal-energy expression is reduced to the change $w(\mathbf{R}-\mathbf{R}') \to w_{\text{tot}}(\mathbf{R}-\mathbf{R}')$ and, thus, to the change of corresponding Fourier components $\hat{w}(\mathbf{k}) \to \hat{w}_{\text{prm}}(\mathbf{k}) \to \hat{w}_{\text{tot}}(\mathbf{k})$, where

$$\tilde{w}_{\text{tot}}(\mathbf{k}) = \tilde{w}_{\text{prm}}(\mathbf{k}) + \tilde{J}_{\text{NiNi}}(\mathbf{k})s_{\text{Ni}}^2\sigma^2 .$$

Here, Fourier component $\tilde{w}_{\text{prm}}(\mathbf{k})$ of the 'mixing' energies $\{w(\mathbf{R}-\mathbf{R}')\}$ corresponds to the paramagnetic state, $\tilde{J}_{\text{NiNi}}(\mathbf{k}) = \sum_{\mathbf{R}'} J_{\text{NiNi}}(\mathbf{R}-\mathbf{R}')e^{-i\mathbf{k}\cdot(\mathbf{R}-\mathbf{R}')}$ is a Fourier component of exchange integrals $\{J_{\text{NiNi}}(\mathbf{R}-\mathbf{R}')\}$. Thus, taking into account of the magnetism in the internal energy expression reduces to the change of $\tilde{w}(\mathbf{k})$ by $\tilde{w}_{\text{tot}}(\mathbf{k})$.

Within the 'molecular'-field approximation, the magnetic entropy ΔS^0_{magn} is defined as an entropy of the system of non-interacting spin moments, the summation of which is $N_{\text{Ni}}s_{\text{Ni}}\sigma = N_{\text{Ni}}s_T$. The value $N_{\text{Ni}}s_T$ defines the total magnetization of alloy, M_T, at the given temperature T [32]:

$$M_T = N_{\text{Ni}}s_T\mu_B g,$$

where N_{Ni} is the total number of Ni atoms; the Lande factor $g \cong 2.0$. The case when $s_{\text{Ni}} = 1/2$ corresponds to such an Ising model of Ni–Al alloy, if each magnetic Ni atom has one unpaired ('magnetic') electron with spin 'up' or 'down'. Such a model was already used in many works (see, *e.g.*, bibliography in Ref. [32]). The magnetic entropy ΔS^0_{magn} is as follows [32]:

$$\Delta S^{0\frac{1}{2}}_{\text{magn}} \cong -k_B N_{\text{Ni}}\left(\frac{1+\sigma}{2}\ln\frac{1+\sigma}{2} + \frac{1-\sigma}{2}\ln\frac{1-\sigma}{2}\right).$$

The direct expression for the magnetic entropy of the system of moments with spins $s_{\text{Ni}} = 1$ was obtained in Refs. [39, 40]. Authors took into account the 'quantization' rule, according to which, in each of the N_{Ni} sites $\{\mathbf{R}\}$, where the Ni atom is located, the projection of the spin onto the selected direction of magnetization (*e.g.*, *Oz*) is of 1, 0, or –1.

So, the configurational free energy of magnetic Ni–Al alloy, which tends to be ordered by means of the $L1_2$-type (super)structure, has been obtained within the nearest-neighbour exchange-interaction model for $s_{\rm Ni} = 1/2$ and $s_{\rm Ni} = 1$.

If the restrictions of the neatest-neighbour exchange interactions are cancelled, the magnetic entropy is as follows [8, 31, 39]:

$$S_{\rm mag} \cong k_B c_{\rm Ni}\left[\ln \mathrm{sh}\left(\left(1+\frac{1}{2s_{\rm Ni}}\right)y_{\rm Ni}(\sigma)\right) - \ln \mathrm{sh}\left(\frac{y_{\rm Ni}(\sigma)}{2s_{\rm Ni}}\right) - \sigma_{\rm Ni} y_{\rm Ni}(\sigma)\right],$$

where $c_{\rm Ni}$ is Ni-atoms' concentration, $y_{\rm Ni} = (s_{\rm Ni}H_{\rm eff})/(k_BT)$ is the magnetic-to-thermal-energy ratio. The magnetic energy in the numerator is defined by the Weiss 'molecular' field $H_{\rm eff} = -\mu_B g \Gamma_{\rm NiNi}\sigma$ (with Weiss coefficient $\Gamma_{\rm NiNi}$) acting on each spin from other ones and depends in direct proportion to $s_{\rm Ni}$ and the reduced magnetization $\sigma \approx \langle \hat{S}_{\mathbf{R}}\rangle_{\rm sp}/s_{\rm Ni}$ ($|\sigma| \le 1$). Brillouin function reads as follows [35, 41, 42]):

$$B_{s_{\rm Ni}}(y_{\rm Ni}) = \left(1+\frac{1}{2s_{\rm Ni}}\right)\mathrm{cth}\left[\left(1+\frac{1}{2s_{\rm Ni}}\right)y_{\rm Ni}\right] - \frac{1}{2s_{\rm Ni}}\mathrm{cth}\left[\frac{1}{2s_{\rm Ni}}y_{\rm Ni}\right].$$

The self-consistent ('molecular') field approximation results in the following equation for the equilibrium spontaneous magnetization of the magnetic (namely, nickel) subsystem:

$$\sigma \cong B_{s_{\rm Ni}}\left(\frac{s_{\rm Ni}H_{\rm eff}}{k_BT}\right).$$

Therefore, taking into account the magnetism, the specific configurational free energy of the $L1_2$-Ni–Al alloy can be written in terms of the Brillouin function:

$$\frac{\Delta F_{\rm conf}}{k_BTN} \cong \frac{\Delta H_0^{\rm Ni-Al}}{k_BTN} + \frac{c_{\rm Ni}^2}{2k_BT}\left[\tilde{w}_{\rm prm}(\mathbf{0}) + \tilde{J}_{\rm NiNi}(\mathbf{0})s_{\rm Ni}^2\sigma^2\right] +$$

$$+\frac{3\eta^2}{32k_BT}\left[\tilde{w}_{\rm prm}(\mathbf{k}^X) + \tilde{J}_{\rm NiNi}(\mathbf{k}^X)s_{\rm Ni}^2\sigma^2\right] +$$

$$+\frac{1}{4}\left[3\left(c_{\rm Ni}+\frac{\eta}{4}\right)\ln\left(c_{\rm Ni}+\frac{\eta}{4}\right) + 3\left(1-c_{\rm Ni}-\frac{\eta}{4}\right)\ln\left(1-c_{\rm Ni}-\frac{\eta}{4}\right) +\right.$$

$$\left.+\left(c_{\rm Ni}-\frac{3\eta}{4}\right)\ln\left(c_{\rm Ni}-\frac{3\eta}{4}\right) + \left(1-c_{\rm Ni}+\frac{3\eta}{4}\right)\ln\left(1-c_{\rm Ni}+\frac{3\eta}{4}\right)\right] -$$

$$-c_{\rm Ni}\left[\ln \mathrm{sh}\left(\left(1+\frac{1}{2s_{\rm Ni}}\right)y_{\rm Ni}(\sigma)\right) - \ln \mathrm{sh}\left(\frac{y_{\rm Ni}(\sigma)}{2s_{\rm Ni}}\right) - y_{\rm Ni}(\sigma)B_{s_{\rm Ni}}(y_{\rm Ni}(\sigma))\right],$$

where (as mentioned above) $\mathbf{k}_X = 2\pi a_0^{-1}(0;0;1)$, $2\pi a_0^{-1}(0;1;0)$ or $2\pi a_0^{-1}(1;0;0)$, and $\mathbf{k}_\Gamma = 2\pi a_0^{-1}(0;0;0) = 0$.

By analogy, expressions for the specific configurational free energy can be written for two other (f.c.c.-based $L1_0$-type [31] and b.c.c.-based $B2$-type [8]) (super)structures with distribution of substitutional Ni and Al atoms.

Using the conditions $\partial\Delta F_{\text{conf}}/\partial\eta = 0$ and $\partial\Delta F_{\text{conf}}/\partial\sigma = 0$, we obtain the set of two transcendental equations for calculation of the equilibrium values of LRO parameters for magnetic (σ) and atomic (η) subsystems, taking into account their relationship:

$$\sigma \cong B_{s_{\text{Ni}}}\left(-\frac{1}{c_{\text{Ni}}k_BT}\left[\tilde{J}_{\text{NiNi}}(\mathbf{0})c_{\text{Ni}}^2 + \frac{3}{16}\eta^2\tilde{J}_{\text{NiNi}}(\mathbf{k}^X)\right]s_{\text{Ni}}^2\sigma\right),$$

$$\ln\frac{(1-c_{\text{Ni}}-\eta/4)(c_{\text{Ni}}-3\eta/4)}{(1-c_{\text{Ni}}+3\eta/4)(c_{\text{Ni}}+\eta/4)} \cong \frac{\eta}{k_BT}\left[\tilde{w}_{\text{prm}}(\mathbf{k}^X) + \tilde{J}_{\text{NiNi}}(\mathbf{k}^X)s_{\text{Ni}}^2\sigma^2\right].$$

Regarding the bifurcation point, note that, within the range of 22–27 at.% Al, f.c.c.-Ni–Al alloys do not undergo actually an disorder–order phase transformation (1st-order phase transition according to the symmetry change $A1\leftrightarrow L1_2$) at any temperatures, *i.e.*, the ordering point is virtually higher than the melting point or almost coincide with it [4, 43]. Liquid phase crystallizes into the (generally, nonstoichiometric) $L1_2$-Ni_3Al-type structure, which is described by the above-mentioned distribution of probabilities to find Ni (Al) atoms at the sites {**R**}.

Let $1 > c_{\text{Ni}} > 3/4$ for $L1_2$-Ni–Al alloy. If we assume that the 'low-temperature' state of the f.c.c.-Ni–Al alloy ($1 > c_{\text{Ni}} > 3/4$) is characterized by the ultimate (for a given c_{Ni}) LRO parameter $\eta \approx 4(1 - c_{\text{Ni}})$, then,

$$\sigma \cong B_{s_{\text{Ni}}}\left(-\frac{1}{c_{\text{Ni}}k_BT}\left[\tilde{J}_{\text{NiNi}}(\mathbf{0})c_{\text{Ni}}^2 + 3(1-c_{\text{Ni}})^2\tilde{J}_{\text{NiNi}}(\mathbf{k}^X)\right]s_{\text{Ni}}^2\sigma\right).$$

Expanding the Brillouin function in a series by powers of y_{Ni} (small near the Curie point T_C for the magnetic–paramagnetic transition) and linearizing it by small σ, we obtain an expression for the Curie temperature of $L1_2$-Ni–Al alloy tending to be ordered [32]:

$$T_C \cong -A_{s_{\text{Ni}}}\frac{\tilde{J}_{\text{NiNi}}(\mathbf{0})c_{\text{Ni}}^2 + 3\eta^2\tilde{J}_{\text{NiNi}}(\mathbf{k}^X)/16}{k_Bc},$$

where, taking into account that $s_{\text{Ni}} = 1/2$ or $s_{\text{Ni}} = 1$, $A_{s_{\text{Ni}}} \equiv (s_{\text{Ni}} + 1) \times \times s_{\text{Ni}}/3 = 1/4$ or $A_{s_{\text{Ni}}} \equiv (s_{\text{Ni}} + 1)s_{\text{Ni}}/3 = 2/3$, respectively. For as much as possible ordered alloy with such a structure, the concentration dependence of the Curie temperature is as follows:

$$T_C \cong -A_{s_{\text{Ni}}}\frac{\tilde{J}_{\text{NiNi}}(\mathbf{0})c_{\text{Ni}}^2 + 3(1-c_{\text{Ni}})^2\tilde{J}_{\text{NiNi}}(\mathbf{k}^X)}{k_Bc_{\text{Ni}}}.$$

Then, the equations for magnetization are transformed into one special equation of the equilibrium state for spontaneous magnetization [35]:

$$\sigma \cong B_{s_{\rm Ni}}\left(-\frac{s_{\rm Ni}^2}{A_{s_{\rm Ni}}}\frac{T_C}{T}\sigma\right),$$

which transforms into known equations [34] for determination of the dependence of the reduced spontaneous magnetization on the reduced temperature T/T_C:

$$\left(\frac{1}{2\sigma}\ln\frac{1+\sigma}{1-\sigma}\right)^{-1} \cong \frac{T}{T_C},\ \text{if}\ \ s_{\rm Ni}=\frac{1}{2};$$

$$\frac{3\sigma}{2}\left[\ln\frac{\sigma+\sqrt{4-3\sigma^2}}{2(1-\sigma)}\right]^{-1} \cong \frac{T}{T_C},\ \text{if}\ \ s_{\rm Ni}=1.$$

It is possible to verify the acceptability of the following sufficiently good approximate analytical expression for the description of such equally important dependences:

$$\sigma_{\rm eq} \cong \left(1-\frac{T}{T_C}\right)^{1/2}\left(1+K\frac{T}{T_C}\right),$$

where $K \approx 0.73$ for $s_{\rm Ni} = 1/2$, whereas $K \approx 0.648$ for $s_{\rm Ni} = 1$ [39]. Regarding the fitting parameter K, we have to note that it makes sense to select K from the range 0.5–0.74. For K smaller than 0.5, this approximate dependence $\sigma_{\rm eq} = \sigma_{\rm eq}(T/T_C)$ deviates significantly from the numerical solution; for K larger than 0.74, an approximate estimate of $\sigma_{\rm eq}$ can lead to overestimation of values (over 1) in the intermediate temperature range.

4. Estimation of Exchange Interaction Parameters

Equations from previous section shown that thermodynamic properties of magnetic alloys tending towards $L1_2$-type ordering, under the influence of nearest-neighbour exchange interaction between Ni atoms, are determined by four energy parameters: $\tilde{w}_{\rm prm}(\mathbf{0})$, $\tilde{w}_{\rm prm}(\mathbf{k}^X)$, $\tilde{J}_{\rm NiNi}(\mathbf{0})$, and $\tilde{J}_{\rm NiNi}(\mathbf{k}^X)$.

As mentioned, the Fourier component of 'mixing' energies, $\tilde{w}(\mathbf{k})$, can be determined from the diffuse scattering of x-rays *via* the Krivoglaz–Clapp–Moss formula $I_{\rm SRO} = I_{\rm SRO}(\mathbf{q}) \cong f(\tilde{w}(\mathbf{k}))$ [44, 45]. This formula relates $\tilde{w}(\mathbf{k})$ with the diffuse-scattering intensity ($I_{\rm SRO}$) of the disordered solid A–B solution caused by the SRO and measured at temperature T in the point $\mathbf{q} = \mathbf{B} + \mathbf{k}$ located at the distance $\mathbf{k}$ from the nearest 'site' $\mathbf{B}$ of the reciprocal space. There are two possibilities herewith. If an equilibrium SRO corresponds to the paramagnetic region of the state dia-

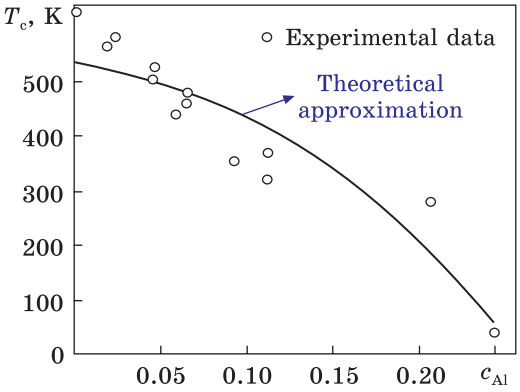

Fig. 4. Concentration-dependent Curie temperature $T_C(c_{Al})$ of the magnetic phase transition in f.c.c. Ni–Al alloys: ○ — experimental data (see Ref. [47] and Refs. therein); solid line — approximation (fitting) curve according to the obtained expression for T_C

gram ($T > T_C$), the value of $\tilde{w}(\mathbf{k})$ in the Krivoglaz–Clapp–Moss formula is $\tilde{w}_{prm}(\mathbf{k})$. If the equilibrium SRO corresponds to the ferromagnetic region ($T < T_C$), $\tilde{w}(\mathbf{k})$ is $\tilde{w}_{tot}(\mathbf{k}) = \tilde{w}_{prm}(\mathbf{k}) + \tilde{w}_{magn}(\mathbf{k})$.

The parameters $\tilde{w}_{tot}(\mathbf{k})$ are not constant. In the ferromagnetic state, the value of $\tilde{w}_{magn}(\mathbf{k}) = \tilde{J}_{NiNi}(\mathbf{0})s_{Ni}^2\sigma^2$ depends on the temperature and composition, first of all, through the squared magnetization. In addition, due to the dependence of exchange integrals on the interatomic distance (in particular, $J_{NiNi}(r) \propto 1/r^{9/2}$ [6] in the three-dimensional lattice), the implicit temperature and concentration dependences of $\tilde{J}_{NiNi}(\mathbf{k})$ due to the thermal and concentration expansions of the lattice can also occur. Thus, depending on the temperature, the Krivoglaz–Clapp–Moss formula allows estimating either $\tilde{w}_{prm}(\mathbf{k})$ (if $T > T_C$) or $\tilde{w}_{tot}(\mathbf{k})$ (if $T < T_C$). The difference between these two values is $\tilde{J}_{NiNi}(\mathbf{0})s_{Ni}^2\sigma^2$ that corresponds to lower temperature ($T < T_C$). This circumstance opens up opportunities for experimental estimation of quantities $\tilde{J}_{NiNi}(\mathbf{k})$ for different $\mathbf{k}$. After evaluating them, it will be possible to find out exchange integrals, $J_{NiNi}(r)$, for different distances r in the lattice. This would be an important result (obviously, not realizable by other methods). To perform this task, it is necessary to carry out very sharp tempering of the alloy relative to the magnetic region.

The values of $A_{s_{Ni}}\tilde{J}_{NiNi}(\mathbf{0})$ and $A_{s_{Ni}}\tilde{J}_{NiNi}(\mathbf{k}^X)$ can be estimated through the optimization procedure using the literature data (see Refs. in the review [32]) on concentration-dependent Curie temperature. To estimate the values of $A_{s_{Ni}}\tilde{J}_{NiNi}(\mathbf{0})$ and $A_{s_{Ni}}\tilde{J}_{NiNi}(\mathbf{k}^X)$ for $s_{Ni} = 1/2$ and 1, we have to use the above-mentioned expression for the Curie temperature and experimental values of T_C obtained for both the partially ordered alloy and the most ordered one at given composition. In the first case, the value of η can be approximately estimated, while in the second case, the LRO parameter η is assumed to be equal to $4(1 - c_{Ni})$.

Authors of Ref. [47] used experimental data on the concentration-dependent T_C for f.c.c.-Ni–Al (Fig. 4) and estimated the Fourier para-

meters of the short-range exchange interaction between Ni moments $A_{s_{\rm Ni}}\tilde{J}_{\rm NiNi}(\mathbf{0})$ and $A_{s_{\rm Ni}}\tilde{J}_{\rm NiNi}(\mathbf{k}^X)$ as well as corresponding values of exchange integrals $J_{\rm NiNi}(r_{\rm I})$ and $J_{\rm NiNi}(r_{\rm II})$ in the real space within the first two co-ordination shells. As seen from Table 1, for both spins $s_{\rm Ni} = 1/2$ and 1, exchange integrals correspond to ferromagnetic character of Ni-atoms' interaction on the distance of the first (I) co-ordination shell, whereas to antiferromagnetic one on the Ni–Ni-distance of the second (II) co-ordination shell.

The values of $\tilde{J}_{\rm NiNi}(\mathbf{0})s^2_{\rm Ni}$ estimated from the measuring the energy of magnons at small $\mathbf{k}$ [46] better agree with estimations of $\tilde{J}_{\rm NiNi}(\mathbf{0})s^2_{\rm Ni}$ found out accordingly to the experimental Curie points for $s_{\rm Ni} = 1/2$. Although generally such estimates show that the above-mentioned methods of estimating the magnetic-energy parameter $\tilde{J}_{\rm NiNi}(\mathbf{0})s^2_{\rm Ni}$ agree with each other only qualitatively, it follows from them that the model of localized magnetic moments, which corresponds to the spin $s_{\rm Ni} = 1/2$, describes the exchange interactions more correctly for f.c.c.-Ni–Al alloy, than the model with $s_{\rm Ni} = 1$. Qualitative agreement of the value $\tilde{J}_{\rm NiNi}(\mathbf{0})s^2_{\rm Ni}$ calculated from the spectrum of spin waves within the model of exchange interaction of nearest neighbours, on the one hand, with the value $\tilde{J}_{\rm NiNi}(\mathbf{0})s^2_{\rm Ni}$ estimated from experimental Curie points, which does not include the assumption of exchange interaction of only nearest neighbours, on the other hand, indicates a greater reliability of the latter.

To estimate the Fourier components $\tilde{J}_{\rm NiNi}(\mathbf{k})$ of the exchange-interaction integrals for arbitrary $\mathbf{k}$ points of the reciprocal space, let us use the approximate expression for it through $J_{\rm NiNi}(r_{\rm I})$ and $J_{\rm NiNi}(r_{\rm II})$ within the two co-ordination shells (Table 1) in a real space:

$$\tilde{J}_{\rm NiNi}(\mathbf{k}) \cong 4J_{\rm NiNi}(r_{\rm I})\left[\cos\left(\frac{a_0}{2}k_x\right)\cos\left(\frac{a_0}{2}k_y\right)+\cos\left(\frac{a_0}{2}k_y\right)\cos\left(\frac{a_0}{2}k_z\right)+\right.$$

$$\left.+\cos\left(\frac{a_0}{2}k_z\right)\cos\left(\frac{a_0}{2}k_x\right)\right]+2J_{\rm NiNi}(r_{\rm II})\left[\cos(a_0k_x)+\cos(a_0k_y)+\cos(a_0k_z)\right],$$

where k_x, k_y, k_z are the Cartesian components of the wave vector $\mathbf{k}$ in the reciprocal space of f.c.c. lattice within the first *BZ*. By plotting the

Table 1. **Fourier components $\tilde{J}_{\rm NiNi}(\mathbf{k})$ ($\mathbf{k} = \mathbf{0}$, $\mathbf{k}^X$) and corresponding Fourier originals $J_{\rm NiNi}(r_n)$ of the exchange integrals of interaction between the magnetic moments of Ni atoms in f.c.c. Ni–Al for two nearest-neighbour co-ordination shells (n = I, II)**

Spin quantum number	$\tilde{J}_{\rm NiNi}(0)$, meV	$\tilde{J}_{\rm NiNi}(\mathbf{k}^X)$, meV	$J_{\rm NiNi}(r_{\rm I})$, meV	$J_{\rm NiNi}(r_{\rm II})$, meV
$s_{\rm Ni} = 1/2$	−185.20	478.94	−41.51	52.15
$s_{\rm Ni} = 1$	−69.45	179.60	−15.57	19.56

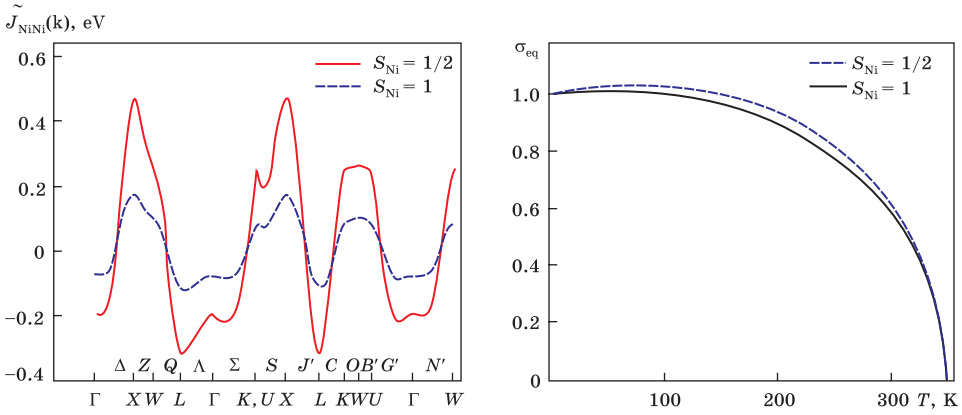

Fig. 5. Dispersion curves of the Fourier components $\tilde{J}_{NiNi}(\mathbf{k})$ of (magnetic) exchange interaction for high-symmetry points of the first Brillouin zone of f.c.c.-Ni–Al lattice for two values of spins of Ni atoms: $s_{Ni} = 1/2$ and 1 [32]

Fig. 6. Approximating temperature-dependent reduced (*i.e.*, per atom) magnetization $\sigma_{eq}(T)$ of Ni–9 at.% Al alloy for two spin 'states' of Ni with $s_{Ni} = 1/2$ or 1 [47]

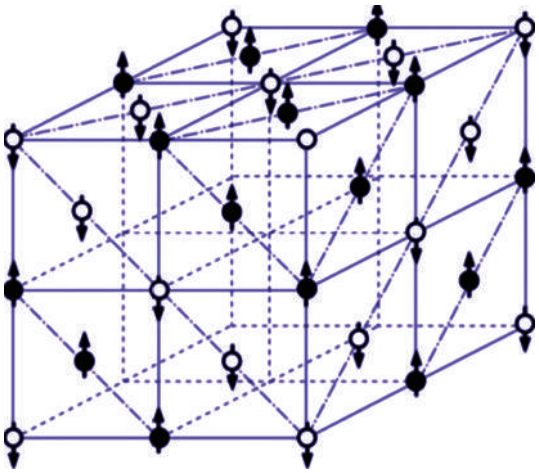

Fig. 7. Hypothetical $L1_1$-type distribution of atoms, which are carriers of magnetic moments, over the sites of f.c.c.-lattice [48], when $\tilde{w}_{prm}(\mathbf{k}) \equiv 0$, *i.e.*, neglecting paramagnetic interactions; here, ○ and ● denote atomic moments with the spin orientation 'down' (↓) and 'up' (↑) in the (½11)-type planes

dispersion curves of the dependence of $\tilde{J}_{NiNi}(\mathbf{k})$ in Fig. 5 for high-symmetry points and directions within the first *BZ*, it is possible to calculate the Fourier components $\tilde{J}_{NiNi}(\mathbf{0})s^2_{Ni}$ of the magnetic-interaction energies for Ni–Ni pairs of atoms. The fact that the approximation of the exchange magnetic interaction by means of the nearest neighbours only turns out to be unsatisfactory is evidenced by the presence of the following significant inequalities:

$$\tilde{J}_{NiNi}(\mathbf{k}^L) \cong -6J_{NiNi}(r_{II}) + \ldots \neq 0,\ \tilde{J}_{NiNi}(\mathbf{0}) \neq -3\tilde{J}_{NiNi}(\mathbf{k}^X),$$

$$\tilde{J}_{NiNi}(\mathbf{k}^X) \neq \tilde{J}_{NiNi}(\mathbf{k}^W) \cong -4J_{NiNi}(r_I) + 2J_{NiNi}(r_{II}) + \ldots.$$

The dependences $\sigma_{eq} = \sigma_{eq}(T)$ are depicted in Fig. 6 for f.c.c.-Ni–9 at.% Al solution in two equilibrium states with Ni atoms possessing spin 1/2 or 1. They were obtained through the minimization of the free energy at $\eta \approx 4(1 - c_{Ni})$, *i.e.*, when the transcendental equation for equilibrium spontaneous magnetization becomes valid.

As seen in Fig. 5, the minimum of Fourier component of exchange integrals, $\tilde{\boldsymbol{J}}_{NiNi}(\mathbf{k})$, falls into the high-symmetry point $L(1/2\ 1/2\ 1/2)$ of the *BZ* surface, which would contribute to generation of hypothetical rhombohedral $L1_1$-type structure of atoms, which are carriers of magnetic moments (Fig. 7 [48]). However, the $L1_2$-type (super)structure acts as a characteristic feature, which is determined by the position of the absolute minimum of the Fourier component of the total 'mixing' energies, *i.e.*, the 'paramagnetic' component together with the magnetic one.

Thus, it is expected that the ordering of the system of interacting magnetic moments of Ni atoms somewhat obstructs the long-range atomic order in f.c.c.-Ni–Al alloys.

5. Concluding Remarks

Literature data on the thermodynamics of Ni–Al-based solid solutions were reviewed and analysed that made it possible to outline the current state of problems and existing challenges, and contributed to the development and construction of statistical-thermodynamic models of ordered (super)structures based on a nickel lattice with Al atoms.

The method of static concentration waves predicts possible types of (super)structures of the Ni–Al alloy. The expressions for the probability functions of the distribution of Ni (Al) atoms over the sites of cubic (f.c.c. or b.c.c.) lattices and the corresponding configurational internal energies and entropies (and, therefore, free energies) of the ordering (super)structures of the $L1_2$-, $L1_0$-, and $B2$-types are presented. The interatomic interaction within the all co-ordination shells is taken into account by switching to the Fourier components of 'mixing' energies. The magnetism of Ni atoms and the energy parameters of the exchange Ni–Ni interaction are estimated. As found, in f.c.c.-Ni–Al alloys, the ordering of the subsystem of interacting magnetic moments of Ni atoms somewhat counteracts to the long-range substitutional-atomic order.

Acknowledgements. Authors are grateful to the National Research Foundation of Ukraine (NRFU) for grant support of the project 'Durability Enhancement of Aircraft Metal Materials: Formation of Structural-Phase States and Physical-Mechanical Properties as Affected by the Solid-Solution, Dispersion and Work Hardenings, and Surface Finishing' (State Reg. No. 0123U103378) within the NRFU Competition 'Science for the Recovery of Ukraine in the War and Post-War Periods' (application ID 2022.01/0038; agreement No. 161/0038 as from

01.08.2023). We are obliged to the Armed Forces of Ukraine for providing security made possible to perform this work as a part of the mentioned project.

REFERENCES

1. D.H. Okamoto, Al–Ni (Aluminum–Nickel), *J. Phase Equilibrium*, **14**, No. 2: 257 (1993);
https://doi.org/10.1007/BF02667823
2. D.P. Pope and J.L. Garin, The temperature dependence of the long-range order parameter of Ni3Al, *J. Appl. Crystallogr.*, **10**, Pt. 1: 14 (1977);
https://doi.org/10.1107/S0021889877012709
3. R.W. Cahn, P.A. Siemers, J.E. Geiger, and P. Bardhanm, The order–disorder transformation in Ni_3Al and Ni_3Al Fe alloys—I. Determination of the transition temperatures and their relation to ductility, *Acta Metall.*, **35**, No. 11: 2737 (1987);
https://doi.org/10.1016/0001-6160(87)90273-2
4. F.J. Bremer, M. Beyss, and H. Wenzl, The order–disorder transition of the intermetallic phase Ni_3Al, *Phys. Status Solidi A*, **110**, No. 1: 77 (1988);
https://doi.org/10.1002/pssa.2211100107
5. Max Hansen and Kurt Anderko, *Constitution of Binary Alloys* (New York: McGraw-Hill: 1965).
6. S.V. Kositsyn and I.I. Kositsyna, Phase and structural transformations in the alloys based on monoaluminide of nickel, *Usp. Fiz. Met.*, **9**, No. 2: 195 (2008) (in Russian);
https://doi.org/10.15407/ufm.09.02.195
7. T.M. Radchenko and V.A. Tatarenko, Atomic-ordering kinetics and diffusivities in Ni–Fe permalloy, *Defect Diffus. Forum*, **273–276**: 525 (2008);
https://doi.org/10.4028/www.scientific.net/DDF.273-276.525
8. I.M. Melnyk, T.M. Radchenko, and V.A. Tatarenko, Semi-empirical parameterization of interatomic interactions, which is based on statistical-thermodynamic analysis of data on phase equilibriums in b.c.c.-Fe–Co alloy. I. Primary ordering, *Metallofiz. Noveishie Tekhnol.*, **32**, No. 9: 1191 (2010) (in Ukrainian).
9. H. Thomas, *Zeitschrift für Metallkunde*, **41**: 185 (1950) (in German).
10. H. Thomas, Über Widerstandslegierungen, *Zeitschrift für Physik*, **129**: 219 (1951) (in German);
https://doi.org/10.1007/BF01333398
11. B.G. Livshits and M.P. Ravdel, *Doklady Akad. Nauk SSSR. Ser.: Tekh. Fiz.*, **93**, No. 6: 1033 (1953) (in Russian).
12. B.G. Livshits, *Physical Properties of Metals and Alloys* (Moskva: Mashgiz: 1959 (in Russian).
13. W. Gaudig, P. Okamoto, G. Schans, G. Tromas, and H. Warlimont, *Ordered Alloys: Structure, Applications and Physical Metallurgy: Proc. III. Bolton Landing Conference* (Baton Rouge, Louisiana: Clayton's Publ. Co.: 1970), p. 347.
14. J.E. Spruiell and E.E. Stansbury, X-ray study of short-range order in nickel alloys containing 10.7 and 20.0 at.% molybdenum, *J. Phys. Chem. Solids*, **26**, No.5: 811 (1965);
https://doi.org/10.1016/0022-3697(65)90256-8
15. E. Ruedl, P. Delavignette, and S. Amelinckx, Electron diffraction and electron microscopic study of long- and short-range order in Ni_4Mo and of the substructure resulting from ordering, *Phys. Status Solidi B*, **28**: 305 (1968);
https://doi.org/10.1002/pssb.19680280132

16. A.A. Katsnelson and P.Sh. Dazhaev, *Izv. VUZov SSSR. Ser.: Fiz.*, No. 4: **23** (1970) (in Russian).
17. A.A. Katsnelson, *Izv. VUZov SSSR. Ser.: Fiz.*, No. 10: 17 (1977) (in Russian).
18. A.G. Khachaturyan, *Fiz. Tverd. Tela*, **13**, No. 8: 2417 (1971) (in Russian).
19. V.N. Bugayev, V.G. Gavrilyuk, V.M. Nadutov, and V.A. Tatarenko, Carbon distribution in Fe–Ni–C and Fe–Mn–C with FCC lattice, *Fiz. Met. Metalloved.*, **68**, No. 5: 931 (1989) (in Russian).
20. V.N. Bugayev, V.G. Gavrilyuk, V.M. Nadutov, and V.A. Tatarenko, Carbon distribution in Fe–Ni–C and Fe–Mn–C with FCC lattice, *Phys. Metals Metallogr.*, **68**, No. 5: 93 (1989).
21. T.M. Radchenko, V.A. Tatarenko, and H. Zapolsky, Statistical thermodynamics and ordering kinetics of $D0_{19}$-type phase: application of the models for H.C.P.-Ti–Al alloy, *Solid State Phenom.*, **138**: 283 (2008); https://doi.org/10.4028/www.scientific.net/ssp.138.283
22. T.M. Radchenko, V.A. Tatarenko, H. Zapolsky, and D. Blavette, Statistical-thermodynamic description of the order–disorder transformation of $D0_{19}$-type phase in Ti–Al alloy, *J. Alloys Compd.*, **452**, No. 1: 122 (2008); https://doi.org/10.1016/j.jallcom.2006.12.149
23. T. Radchenko, H. Zapolsky, D. Blavette, and V. Tatarenko, Computation of kinetic and thermodynamic characteristics for close-packed crystalline solutions from diffuse scattering and phase diagram data, *Acta Cryst.*, **A60**: s71 (2004); https://doi.org/10.1107/S0108767304098599
24. E. Hornbogen and M. Roth, Die Verteilung kohärenter Teilchen in Nickellegierungen, *Zeitschrift für Metallkunde*, **58**: 842 (1967) (in German); https://doi.org/10.1515/ijmr-1967-581203
25. V.A. Tatarenko and T.M. Radchenko, Parameters of the short-range order relaxation kinetics and interactions of atoms in binary substitutional f.c.c. solid solutions according to the data about time evolution of diffuse scattering of radiations, *Metallofiz. Noveishie Tekhnol.*, **24**, No. 10: 1335 (2002) (in Ukrainian).
26. D.S. Leonov, T.M. Radchenko, V.A. Tatarenko, and Yu.A. Kunitsky, Kinetic parameters of migration of atoms and relaxation of scattering of different-type waves in the ordering f.c.c.-Ni–Al alloy, *Metallofiz. Noveishie Tekhnol.*, **29**, No. 12: 1587 (2007) (in Russian).
27. D.S. Leonov, T.M. Radchenko, V.A. Tatarenko, and Yu.A. Kunitsky, Kinetics parameters of atomic migration and diffuse scattering of radiations within the f.c.c.-Ni–Al alloys, *Defect Diffus. Forum*, **273–276**: 520 (2008); https://doi.org/10.4028/www.scientific.net/DDF.273-276.520
28. S.M. Bokoch, D.S. Leonov, M.P. Kulish, V.A. Tatarenko, and Yu.A. Kunitsky, Influence of a relaxation of the atomic order in f.c.c.-Ni–Al alloys on x-ray diffuse scattering, electrical resistance and microhardness, *Metallofiz. Noveishie Tekhnol.*, **30**, No. 12: 1677 (2008) (in Russian).
29. S.M. Bokoch, D.S. Leonov, M.P. Kulish, V.A. Tatarenko, and Yu.A. Kunitsky, Influence of relaxation of the atomic order in f.c.c.-Ni–Al alloys on x-ray diffuse scattering, *Phys. Status Solidi A*, **206**, No. 8: 1766 (2009); https://doi.org/10.1002/pssa.200881604
30. V.A. Tatarenko and T.M. Radchenko, Direct and indirect methods of the analysis of interatomic interaction and kinetics of a relaxation of the short-range order in close-packed substitutional (interstitial) solid solutions, *Usp. Fiz. Met.*, **3**, No. 2: 111 (2002) (in Ukrainian); https://doi.org/10.15407/ufm.03.02.111

31. T.M. Radchenko and V.A. Tatarenko, Fe–Ni alloys at high pressures and temperatures: statistical thermodynamics and kinetics of the $L1_2$ or $D0_{19}$ atomic order, *Usp. Fiz. Met.*, **9**, No. 1: 1 (2008) (in Ukrainian); https://doi.org/10.15407/ufm.09.01.001
32. V.A. Tatarenko, O.V. Sobol', D.S. Leonov, Yu.A. Kunyts'kyy, and S.M. Bokoch, Statistical thermodynamics and physical kinetics of structural changes of quasi-binary solid solutions based on the close-packed simple lattices (according to the data about evolution of a pattern of scattering of waves of various kinds), *Usp. Fiz. Met.*, **12**, No. 1: 1 (2011) (in Ukrainian); https://doi.org/10.15407/ufm.12.01.001
33. V.A. Tatarenko and C.L. Tsynman, Strain-induced and blocking effects in thermodynamics of the ordering and precipitation reactions within the off-stoichiometric close-packed-metal hydrides, *Solid State Ionics*, **101–103**: 1061 (1997); https://doi.org/10.1016/s0167-2738(97)00376-7
34. A.G. Khachaturyan, *Theory of Structural Transformations in Solids* (Mineola, NY: Dover Publications, Inc.: 2008).
35. A. Aharoni, *Introduction to the Theory of Ferromagnetism* (New York: Oxford University Press Inc.: 2000).
36. T. Moriya, *Spin Fluctuations in Itinerant Electron Magnetism* (Berlin–Heidelberg: Springer-Verlag: 1985).
37. J. Kübler, *Theory of Itinerant Electron Magnetism* (New York: Oxford University Press Inc.: 2009).
38. P. Mohn, *Magnetism in the Solid State: An Introduction* (Berlin–Heidelberg: Springer-Verlag: 2003).
39. S.V. Semenovskaya, The application of x-ray diffuse scattering to the calculation of the Fe–Al equilibrium diagram, *Phys. Status Solidi B*, **64**, No. 1: 291 (1974); https://doi.org/10.1002/pssb.2220640134
40. G. Inden, The role of magnetism in the calculation of phase diagrams, *Physica B*, **103**, No. 1: 82 (1981); https://doi.org/10.1016/0378-4363(81)91004-4
41. J.S. Smart, *Effective Field Theories of Magnetism* (Philadelphia: Saunders: 1966).
42. M.I. Darby, Tables of the Brillouin function and of the related function for the spontaneous magnetization, *British J. Appl. Phys.*, **18**, No. 10: 1415 (1967); https://doi.org/10.1088/0508-3443/18/10/307
43. H.Y. Geng, M.H.F. Sluiter, and N.X. Chen, Order–disorder effects on the equation of state for fcc Ni–Al alloys, *Phys. Rev. B*, **72**: No. 1: 014204 (2005); https://doi.org/10.1103/PhysRevB.72.014204
44. M.A. Krivoglaz, *Zh. Eksp. Teor. Fiz.*, **32**, No. 6: 1368 (1957) (in Russian).
45. P.C. Clapp and S.C. Moss, Correlation functions of disordered binary alloys. I, *Phys. Rev.*, **142**: 418 (1966); https://doi.org/10.1103/PhysRev.142.418
46. A. Semwal and S.N. Kaul, Low-lying magnetic excitations in Ni_3Al and their suppression by a magnetic field, *Phys. Rev. B*, **60**, No. 18: 12799 (1999); https://doi.org/10.1103/PhysRevB.60.12799
47. V.A. Tatarenko, V.V. Odnosum, Yu.M. Koval', and G.E. Monastyrs'ky, Magnetic interatomic interactions and atomic ordering in nonstoichiometric $L1_2$-type Ni–Al alloys, *Metallofiz. Noveishie Tekhnol.*, **25**, No. 9: 1111 (2003) (in Russian).

48. A.G. Khachaturyan, Ordering in substitutional and interstitial solid solutions, *Progr. Mater. Sci.*, **22**, Nos. 1–2: 1 (1978); https://doi.org/10.1016/0079-6425(78)90003-8

Received 17.11.2023
Final version 01.12.2023

В.А. Татаренко, Т.М. Радченко, А.Ю. Наумук, Б.М. Мордюк
Інститут металофізики ім. Г.В. Курдюмова НАН України,
бульв. Академіка Вернадського, 36,
03142 Київ, Україна

СТАТИСТИЧНО-ТЕРМОДИНАМІЧНІ МОДЕЛІ УПОРЯДКОВНИХ ФАЗ ($L1_2$, $L1_0$, $B2$) НА ОСНОВІ Ni–Al: РОЛЬ МАГНЕТНОГО ВНЕСКУ АТОМІВ Ni

Серед відомих авіаційних металевих матеріалів Ni–Al ідентифіковано як упорядковний інтерметалевий стоп із кількома привабливими властивостями, в тому числі низькою густиною (≅6 г/см^3), високою температурою топлення (≅1911 К), відмінною стійкістю щодо окиснення (до 1573 К) і гарною теплопровідністю. Ці та інші фізичні властивості зумовлено не лише хемічним складом, але й розподілом атомів по вузлах кристалічної ґратниці. Взаємодії між атомами різного сорту приводять до відхилів від випадкового розподілу їх і виникнення близького (кореляційного) або навіть далекого (як у випадку Ni–Al) порядків. В даній роботі проаналізовано можливі типи упорядковних фаз стопів Ni–Al завдяки одержаним виразам для ймовірнісних функцій розподілу атомів Ni (Al) по вузлах ГЦК- й ОЦК-ґратниць. В одержаних виразах для конфіґураційної вільної енергії упорядковних структур типу $L1_2$, $L1_0$ і B_2 враховано взаємодію атомів заміщення на усіх (а не лише найближчих) координаційних сферах і магнетизм атомів Ni. За оцінкою енергетичних параметрів обмінної Ni–Ni-взаємодії встановлено, що у ГЦК-Ni–Al упорядкування системи взаємодійних магнетних моментів атомів Ni деяк перешкоджає далекому порядку.

Ключові слова: Ni–Al, статистична термодинаміка, далекий атомовий порядок, енергія «змішання», обмінна взаємодія, намагнетованість.